Amplitude reduction of waviness in elastohydrodynamic lubrication using an Eyring fluid model

B Jacod[1]*, **P M Lugt**[2], **M L Dumont**[2], **J H Tripp**[2] and **C H Venner**[1]
[1]Department of Mechanical Engineering, University of Twente, Enschede, The Netherlands
[2]SKF Engineering and Research Centre BV, Nieuwegein, The Netherlands

Abstract: This paper presents a first extension of the amplitude reduction approach, where the deformation of harmonic components of the roughness is considered, to non-Newtonian elastohydrodynamic lubrication (EHL) line contact. The amplitude reduction of one-sided waviness is computed as a function of the slide–roll ratio. Non-Newtonian effects result in an increase in the deformation for positive slide–roll ratios. This contrasts with published results using a Newtonian fluid where the deformation decreased for such conditions. Moreover, the amplitude reduction varies significantly throughout the contact, requiring an additional parameter for the characterization of the amplitude reduction. An explanation of these differences based on the velocity profile of the lubricant inside the contact concludes the paper.

Keywords: transient elastohydrodynamic lubrication (EHL), one-sided roughness, non-Newtonian

NOTATION

A	amplitude of the surface feature
$\mathscr{A}$	dimensionless amplitude $= AR/b^2$
$\mathscr{A}_i$	dimensionless initial amplitude
$\mathscr{A}_d$	dimensionless deformed amplitude
b	half-width Hertzian contact $= \sqrt{8wR/(\pi E')}$
E'	reduced elasticity modulus, $2/E' = (1 - \nu_1^2)/E_1 + (1 - \nu_2^2)/E_2$
h	film thickness
H	dimensionless film thickness $= hR/b^2$
H_0	constant
L	dimensionless material parameter (Moes) $= \alpha E'[\eta_0 u_s/(E'R_x)]^{1/4}$
M	dimensionless load parameter (Moes) $= [w/(E'R_x^2)][E'R_x/(\eta_0 u_s)]^{3/4}$
p	pressure
p_H	maximum Hertzian pressure $= 2w/(\pi b)$
P	dimensionless pressure $= p/p_H$
R	reduced radius of curvature, $R^{-1} = R_1^{-1} + R_2^{-1}$
$\mathscr{R}$	expression of the roughness
$\mathscr{S}$	slide–roll ratio $= (u_2 - u_1)/\overline{u}$
t	time
T	dimensionless time $= u_s t/2b$
u	velocity
$\overline{u}$	average velocity $= (u_1 + u_2)/2$

u_L	lubricant velocity in the contact zone
u_s	sum velocity $= u_1 + u_2$
w	external load per unit width
x	coordinate
X	dimensionless coordinate $= x/b$
X_a, X_b	dimensionless position of the the boundaries
X_d	position of the start of the surface waviness
z, Z'	coordinates
α	pressure–viscosity index
ϵ	coefficient $= \overline{\rho}H^3/(\overline{\eta}\overline{\lambda})$
η	viscosity
η_0	viscosity at ambient pressure
$\overline{\eta}$	dimensionless viscosity $= \eta/\eta_0$
$\overline{\lambda}$	dimensionless speed parameter $= 6\eta_0 u_s R^2/(b^3 p_H)$
λ, λ'	wavelengths of the waviness
ρ	density
ρ_0	density at ambient pressure
$\overline{\rho}$	dimensionless density $= \rho/\rho_0$
Σ	dimensionless function
τ_{xz}	shear stress
τ_0	Eyring stress
τ_m	mid-plane shear stress

Subscripts

1, 2	bodies 1 and 2 respectively (body 1 is smooth)
min	minimum
max	maximum

1 INTRODUCTION

In recent years, the focus has moved from the study of smooth elastohydrodynamically lubricated (EHL) contacts to more complex configurations where the effects of surface roughness, lubricant behaviour and temperature are gradually introduced. This trend reflects an increasing severity of the operating conditions in real-life applications as well as the development of solvers fast and stable enough to tackle this complexity. The decrease in the thickness of the lubricant film results in a growing importance of surface topography. Meanwhile the failure of simulations based on the Newtonian model to predict traction correctly has emphasized the need for more realistic lubricant models.

Soon after the development of solvers for the smooth non-Newtonian EHL contact [1–4], the analysis of surface roughness and non-Newtonian behaviour was combined. The influence of non-Newtonian behaviour on the deformation of simple features like bumps and waviness was considered first [5–7].

In parallel, the introduction of the amplitude reduction approach applied to harmonic components of the surface roughness enabled considerable progress to be made in the understanding of roughness deformation in EHL conjunctions. Line and point contacts for both pure rolling and sliding configurations have been considered but with a Newtonian lubricant only [8, 9].

This paper presents a first step towards the extension of the amplitude reduction approach to non-Newtonian line contacts. The deformation of one-sided waviness going through the EHL conjunction is calculated as a function of the slide–roll ratio. The results presented here are compared with those given by Lubrecht et al. [9] where the same configuration is studied using the Newtonian model. The differences are significant, the reduction in amplitude showing quite opposite trends for $\mathscr{S} > 0$. A discussion of the results based on the velocity distribution across the lubricant film in the length of the contact concludes the paper.

2 THEORY

2.1 Rheological models

Under the severe conditions occurring in an EHL conjunction, most lubricants exhibit non-Newtonian behaviour [10]. Several models have been proposed to describe this non-linear behaviour, among which stands the Eyring model:

$$\frac{\partial u}{\partial z} = \frac{\tau_0}{\eta} \sinh\left(\frac{\tau_{xz}}{\tau_0}\right) \qquad (1)$$

An Eyring fluid was first used by Johnson and Tevaarwerk [11] for predicting traction and has since been used

extensively for this purpose [12]. It has also been used for numerical simulations concerned with the effect of non-Newtonian behaviour on the film thickness and pressure profile of smooth and rough surfaces [2, 5–7]. In this case, a modified Reynolds equation is derived (see, for example, reference [2]), where non-Newtonian effects are incorporated by means of a factor S_e:

$$S_e(x) = \frac{3(\sinh \Sigma - \Sigma \cosh \Sigma)}{-\Sigma^3} \cosh\left(\frac{\tau_m}{\tau_0}\right) \qquad (2)$$

where $\Sigma = (h/2\tau_0)(\partial p/\partial x)$ and the mean shear stress is given by

$$\sinh\left(\frac{\tau_m}{\tau_0}\right) = \frac{\eta(u_2 - u_1)}{\tau_0 h} \frac{\Sigma}{\sinh\Sigma} \qquad (3)$$

As τ_0 approaches infinity, S_e approaches unity and the Eyring model turns into the Newtonian model. Moreover, under pure rolling conditions, S_e remains small in the central part of the contact where the lubricant behaviour is thus approximately Newtonian, non-Newtonian effects being, however, present in the pressure spike region. The behaviour of the fluid reverts to Newtonian if S_e is taken equal to 1.

2.2 Equations

The modified Reynolds equation is made dimensionless using the Hertzian dry contact parameters:

$$\frac{\partial}{\partial X}\left(\epsilon S_e \frac{\partial P}{\partial X}\right) - \frac{\partial \overline{\rho} H}{\partial X} - \frac{\partial \overline{\rho} H}{\partial T} = 0 \qquad (4)$$

The boundary conditions are $P(X_a, T) = P(X_b, T) = 0$, $\forall T$ where X_a and X_b denote the boundaries of the domain. Furthermore, the cavitation condition $P(X, T) \geqslant 0, \forall X, T$ must be satisfied. ϵ and $\overline{\lambda}$ are defined according to

$$\epsilon = \frac{\overline{\rho} H^3}{\overline{\eta}\overline{\lambda}}, \quad \overline{\lambda} = \frac{12\eta_0 \overline{u} R^2}{b^3 p_H} \qquad (5)$$

The density–pressure relation is given by the Dowson–Higginson [13] relation and the viscosity–pressure relation by the Roelands [14] relation. The film thickness equation is

$$H(X, T) = H_0(T) + \frac{X^2}{2} - \mathscr{R}(X, T)$$

$$- \frac{1}{\pi}\int_{X_a}^{X_b} P(X', T)\ln|X - X'| \, \mathrm{d}X' \qquad (6)$$

where $\mathscr{R}(X, T)$ denotes the undeformed waviness geometry:

$$\mathscr{R}(X, T) = \mathscr{A}(X, T) \cos\left(2\pi \frac{X - X_d}{\lambda/b}\right) \qquad (7)$$

where

$$\mathscr{A}(X, T) = \mathscr{A}_i 10^{-10\max[0, (x - x_d)/(\lambda/b)]^2} \qquad (8)$$

The exponential term in the amplitude smoothly suppresses the waviness for $X - X_d \geqslant 0$. The waviness thus starts effectively at $X_d = X_{d,0} + 2Tu_2/u_s$ and therefore allows the computations to start well outside the contact, the waviness moving into the contact with time.

At all times, the load is assumed to be constant. Hence, surface irregularities are assumed not to excite the rolling elements. This condition determines the value of the constant H_0 from equation (6):

$$\int_{X_a}^{X_b} P(X, T)\, dX = \frac{\pi}{2}, \quad \forall T \qquad (9)$$

These equations are discretized up to second order with respect to both space and time. A solver based on multi-grid techniques was used [15–17].

As mentioned before, the work described in this paper is focused on the calculation of the amplitude of the deformed waviness $\mathscr{A}_d$, with initial amplitude $\mathscr{A}_i$, inside the Hertzian contact area. This $\mathscr{A}_d$ has been defined by Venner et al. [8] as the variations in the amplitude of the film thickness with time after these variations have become periodic, i.e. enough time has passed to reach a stable situation:

$$\mathscr{A}_d(X) = \frac{H_{\max T}(X, T) - H_{\min T}(X, T)}{2} \qquad (10)$$

The variable monitored in this work is the relative amplitude $\mathscr{A}_d/\mathscr{A}_i$, the ratio of the deformed amplitude to the out-of-contact amplitude. Note that the relative amplitude increases when the deformation of the waviness decreases.

3 RESULTS

3.1 Operating conditions

The operating conditions are presented in Table 1. They are chosen equal to those taken by Lubrecht et al. [9] to allow comparison. The computational domain is taken as $-2.5 \leqslant X \leqslant 1.5$ with 1025 discretization points. For such a discretization and under the operating conditions considered the numerical accuracy is roughly 1 per cent.

The waviness is present on the upper surface only while the lower surface remains perfectly smooth. Its initial amplitude is one-tenth of the central film thickness in the

Table 1 Operating conditions

M	100
L	11.08
α	2.2×10^{-8} Pa^{-1}
η_0	0.04 Pa s
τ_0	5 MPa
p_H	2.01 GPa

smooth case, $\mathscr{A}_i = 1.42 \times 10^{-3}$. The amplitude reduction has, however, been proved to be linear in the Newtonian case [8]. Figures 3 and 4 show that this is also the case with a non-Newtonian lubricant; for out-of-contact amplitude as large as one-half of the central film thickness the relative amplitude values differ by less than 5 per cent from those obtained with $\mathscr{A}_i/H_c(\text{smooth}) = 0.1$. It is therefore sufficient to consider small amplitude cases where the numerical accuracy can be well controlled.

3.2 Film thickness and pressure profiles

To study the influence of non-Newtonian rheological behaviour on the reduction in amplitude, the deformation of the waviness inside the contact was calculated for two values of the wavelength as a function of slip. The wavelengths were chosen as $\lambda/b = 1.0$ and $\lambda/b = 0.5$. The slip varies between $\mathscr{S} = -1$ and $\mathscr{S} = 1$, meaning that, for the extreme values, one of the surfaces is moving three times faster than the other.

Figures 1 and 2 show the film thickness and pressure profiles for $\mathscr{S} = 0$ and $\mathscr{S} = 0.6$ and for $\mathscr{S} = 0$ and, $\mathscr{S} = 1$ respectively after the waviness has gone through all the contact. In agreement with published results [5–7, 18], Figs 1 and 2 show that the pressure and film thickness variations are moving with different velocities in the case of slip. This phenomenon has been explained in the case of one-sided waviness by Greenwood and Morales-Espejel [19] and Hooke [20]. The film thickness variations in the inlet are propagated, hardly deformed because of the piezoviscous effect, through the contact with the velocity of
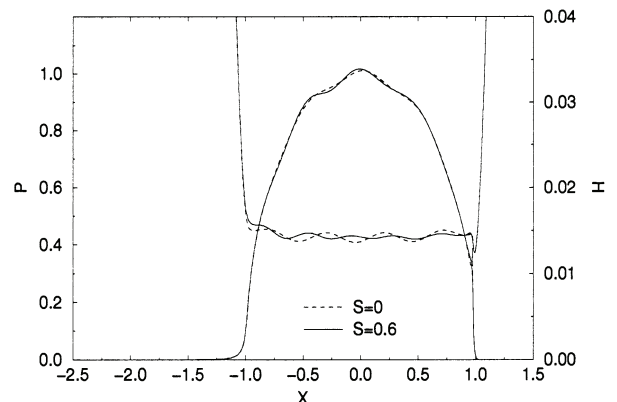

Fig. 1 Film thickness and pressure profile for pure rolling and $\mathscr{S} = 0.6$ [$\mathscr{A}_i/H_c$ (smooth) $= 0.1$ and $\lambda/b = 0.5$]
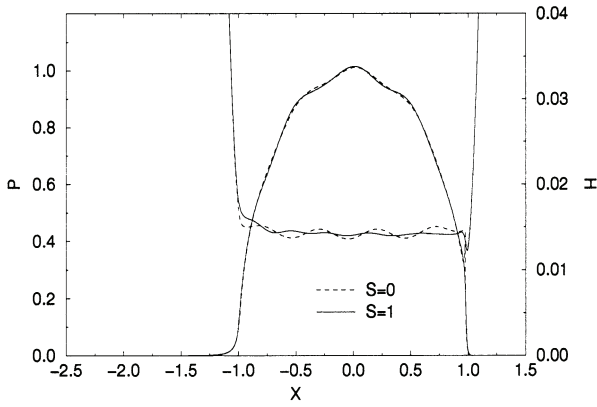
Fig. 2 Film thickness and pressure profile for pure rolling and $\mathscr{S} = 1$ [$\mathscr{A}_i/H_c$ (smooth) $= 0.1$ and $\lambda/b = 0.5$]

the lubricant, u_L. By contrast, the waviness present on the upper surface and the corresponding pressure variations are moving with the upper surface velocity u_2. As a result, Lubrecht [21] has shown that the waviness inside the contact and the out-of-contact waviness have the same frequency but different wavelengths. The wavelength of the film thickness variations in the contact, λ', is related to the out-of-contact wavelength of the waviness, λ, by

$$\frac{\lambda}{u_2} = \frac{\lambda'}{u_L}$$

$$\lambda' = \lambda \frac{u_L}{u_2} \qquad (11)$$

Indeed, for $\mathscr{S} = 1$, Fig. 2 shows clearly that the wavelength of the film thickness variations is smaller than for pure rolling. Another noticeable feature of Figs 1 and 2 is the variation in the amplitude of the waviness throughout the contact for $\mathscr{S} \neq 0$ in contrast with its almost constant value in the pure rolling case. The amplitude is larger close to the inlet than in the outlet. Note that this amplitude is an instantaneous amplitude by contrast with the amplitude defined in equation (10). This feature is studied further in the next section where the amplitude reduction results are presented.

3.3 Amplitude reduction

Figures 3 and 4 show the relative amplitude in the *centre of the contact* as a function of slip for $\lambda/b = 1.0$ and $\lambda/b = 0.5$ respectively. Both figures show that the amplitude reduction reaches a maximum around pure rolling. For $\lambda/b = 1.0$ (Fig. 3), the relative amplitude is increasing if the speed ratio is increasing in the range $-1 \leqslant \mathscr{S} \leqslant 0.2$. It then decreases to reach a minimum for $\mathscr{S} = 1$. For $\lambda/b = 0.5$ (Fig. 4), a similar shape is found again. In this case the decrease in amplitude reduction for $\mathscr{S} \geqslant 0$ is more pronounced. Note that for $\lambda/b = 0.5$ the curve is less smooth than for $\lambda/b = 1.0$ due to the interference between the 'original' waviness λ and the 'induced' waviness λ'.
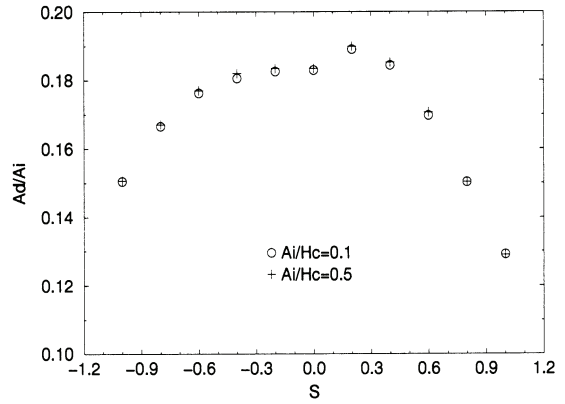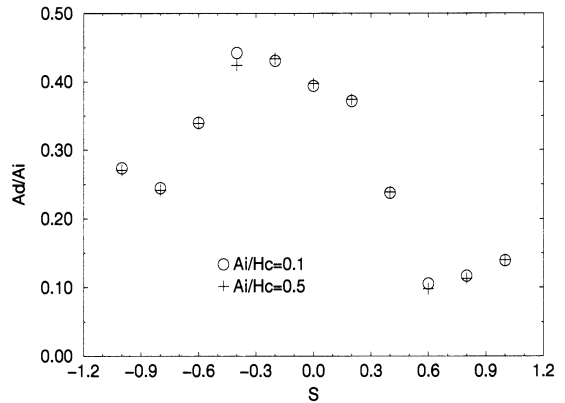

Fig. 3 Relative amplitude of the waviness in the centre of the contact as a function of $\mathscr{S}$ [$\mathscr{A}_i/H_c$ (smooth) $= 0.1$ and 0.5 and $\lambda/b = 1.0$]

Fig. 4 Relative amplitude of the waviness in the centre of the contact as a function of $\mathscr{S}$ [$\mathscr{A}_i/H_c$ (smooth) $= 0.1$ and 0.5 and $\lambda/b = 0.5$]

So far, the amplitude reduction of the waviness has been shown in the centre of the contact only. Figures 5 to 8 show the relative amplitude *throughout the contact* for two (symmetrical) cases with slip and the pure rolling case. From these figures three features of the numerical results are revealed:

1. The relative amplitude $\mathscr{A}_d/\mathscr{A}_i$ is not constant any longer in the length of the contact as soon as $\mathscr{S} \neq 0$. It varies from the inlet to the outlet presenting oscillations which can be clearly seen in Figs 7 and 8.
2. Despite the sometimes large oscillations, a clear trend observed is that the relative amplitude is larger in the inlet than in the outlet. This implies that the waviness is gradually more and more deformed as it moves through the contact.
3. The relative amplitude curves can be grouped as a function of the difference relative to the pure rolling case, $|\mathscr{S}|$, rather than as a function of $\mathscr{S}$ itself. The fact that the upper surface is moving faster or slower than the average velocity seems to be of less importance.
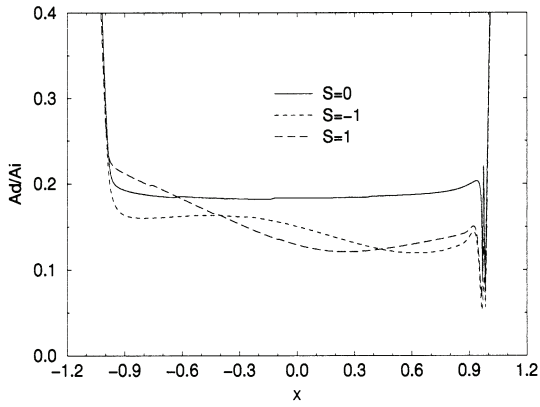
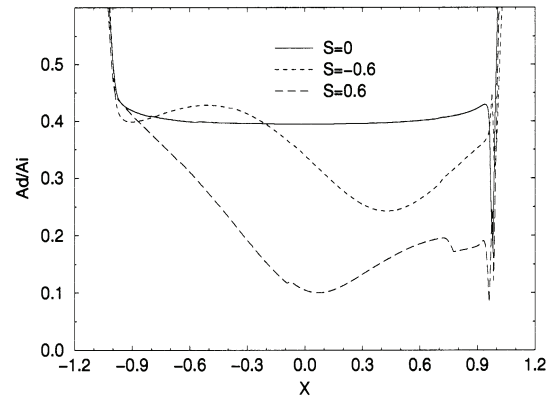**Fig. 5** Relative amplitude for $\mathscr{S} = -1, 1, 0$ and $\lambda/b = 1.0$

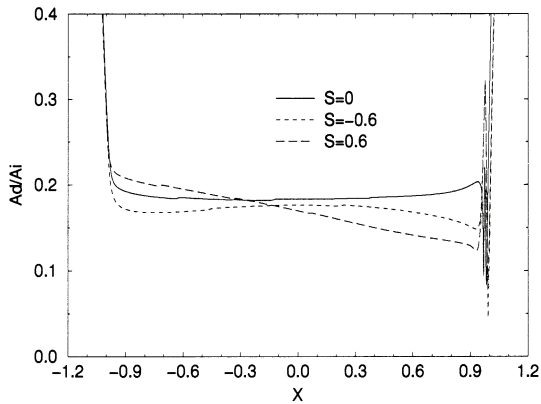**Fig. 6** Relative amplitude for $\mathscr{S} = -0.6, 0.6, 0$ and $\lambda/b = 1.0$

Fig. 7 Relative amplitude for $\mathscr{S} = -1, 1, 0$ and $\lambda/b = 0.5$

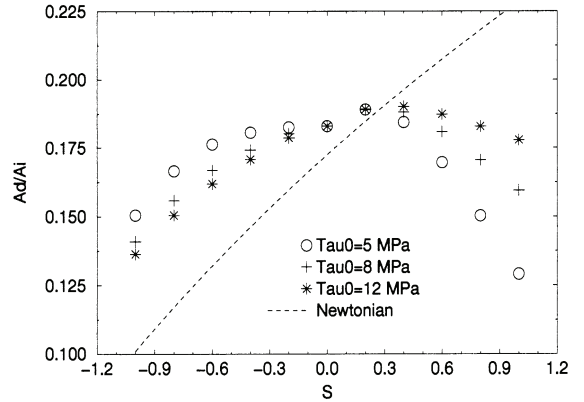**Fig. 8** Relative amplitude for $\mathscr{S} = -0.6, 0.6, 0$ and $\lambda/b = 0.5$

Fig. 9 Relative amplitude of the waviness in the centre of the contact as a function of $\mathscr{S}$ for different values of $\tau_0 (= 5, 8$ and 12 MPa$)$. . . . ., relative amplitude for the Newtonian case as given in reference [9] $(\lambda/b = 1)$
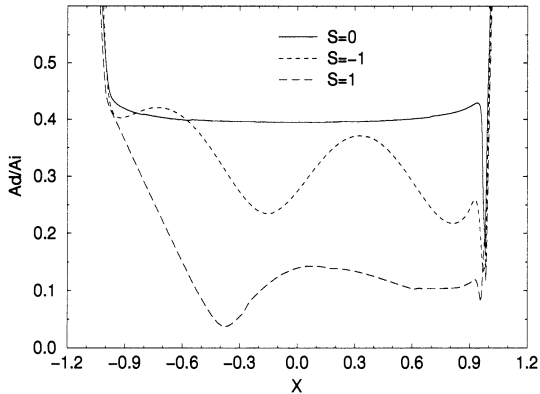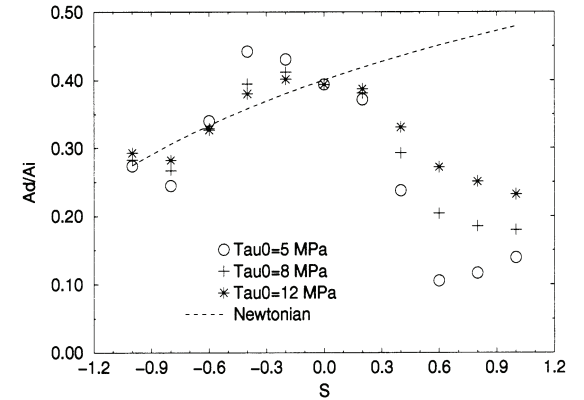

Fig. 10 Relative amplitude of the waviness in the centre of the contact as a function of $\mathscr{S}$ for different values of $\tau_0 (= 5, 8$ and 12 MPa$)$. . . . ., relative amplitude for the Newtonian case as given in reference [9] $(\lambda/b = 0.5)$

These results can be compared with those obtained by Lubrecht *et al.* [9] using a Newtonian model. Calculating the relative amplitude as a function of slip for different wavelengths, they showed that, for the two cases presented here, the relative amplitude was continuously increasing with $\mathscr{S}$. While for $\mathscr{S} \le 0$ the curves are similar, when $\mathscr{S} \ge 0$, their relative amplitude continues to increase with slip using their Newtonian model whereas it decreases when using the Eyring model (see Figs 3 and 4). This difference becomes less significant when non-Newtonian effects become weaker. Figures 9 and 10 show the relative

amplitude in the centre of the contact obtained for different values of τ_0 and as given in the Newtonian case by the formula proposed by Lubrecht *et al.* [9]. With increasing τ_0 the shape of the relative amplitude curve reverts gradually into the Newtonian curve. The decrease in the relative

amplitude characteristic of non-Newtonian results when $\mathscr{S} > 0$ becomes less pronounced with increasing τ_0 for both wavelengths.

4 DISCUSSION

Previous work by Venner *et al.* [8] has established that the amplitude reduction depends on the wavelength of the waviness; large wavelengths are almost completely flattened while small wavelengths are hardly deformed. Moreover, Lubrecht [21] has shown that the wavelength of the waviness inside the contact differs from the out-of-contact wavelength in the case of slip, the in-contact wavelength depending on the lubricant velocity [equation (11)]. In the case of slip, non-Newtonian effects modify the nature of lubricant flow in the contact. The factor S_e in equation (4) prevents the disappearance of the Poiseuille term and the flow now results from the combined effect of the pressure and the shear flow. Non-Newtonian effects may therefore change significantly the velocity profile in the contact and hence the wavelength and deformation of the waviness.

4.1 Non-Newtonian effects on the velocity of the lubricant

The influence of non-Newtonian behaviour on the velocity profile in the contact is therefore studied. Figures 11 and 12 show the position of isovelocity lines in the central region of the contact (see Conry *et al.* [2] for the expression for the velocity). The velocity profiles given by a Newtonian and an Eyring fluid are compared in the smooth case for $\mathscr{S} = 1$ and $\mathscr{S} = -1$. The interval between consecutive lines is one-tenth of $(u_2 - u_1)/(u_2 + u_1)$. These figures show that, with the Newtonian model, the velocity is constant for almost the full length of the contact whereas, for the Eyring model, the velocity clearly changes with X.
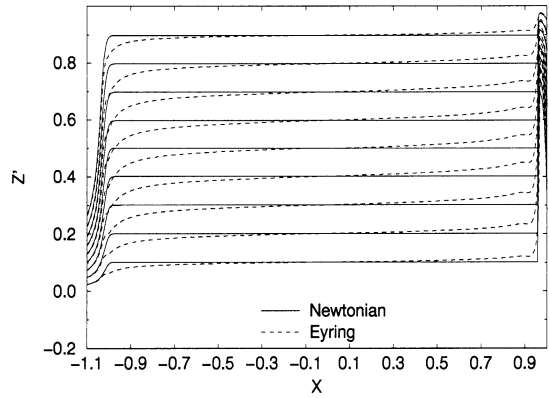
Fig. 12 Isovelocity lines across and through the contact for the Newtonian and Eyring models in the smooth case ($\mathscr{S} = -1$)

If the upper surface is moving faster than the lower surface ($\mathscr{S} = 1$), in the inlet the isovelocity lines obtained with the Eyring model are above those given by the Newtonian model. The velocity is decreasing faster with increasing distance from the upper surface. The lubricant therefore tends to move with a velocity closer to the velocity of the lower surface. In the outlet, on the contrary, the velocity increases faster with increasing distance from the lower surface; the lubricant tends to move with a velocity closer to the upper surface. For $\mathscr{S} = -1$, the opposite is observed; in the inlet, the lubricant film is moving with a velocity closer to the velocity of the upper surface while, in the outlet, the lubricant is moving with a velocity closer to the velocity of the lower surface. Thus, in both cases, the lubricant tends to cling to the slower surface in the inlet and to the faster surface in the outlet.

4.2 Consequences for the deformation of the waviness in the contact

In Section 4.1 it has been established that the lubricant velocity profile, and hence the effective wavelength λ' of the waviness within the contact, depends only on $|\mathscr{S}|$. In non-Newtonian situations, λ' steadily increases from inlet to outlet. For Newtonian cases, which include the Eyring fluid in pure rolling, $\mathscr{S} = 0$, λ' remains essentially constant within the contact. As the fluid enters the contact, its behaviour is still approximately Newtonian, so that the amplitude reduction near $X \leqslant -1$ should be almost rheology independent.

This is confirmed in Figs 5 to 8, where the curves for the two symmetrical sliding situations in all cases lie very close to the Newtonian pure rolling situation. In fact, closer inspection shows that, at $X = -1$, the curves are ordered according to $\mathscr{S}$, i.e. larger u_2 corresponds to larger $\mathscr{A}_d/\mathscr{A}_i$ or smaller amplitude *reduction*. Both here and in reference [9], the amplitude reduction for the Newtonian case shows variations of only a few per cent with X, so that $\mathscr{A}_d/\mathscr{A}_i$
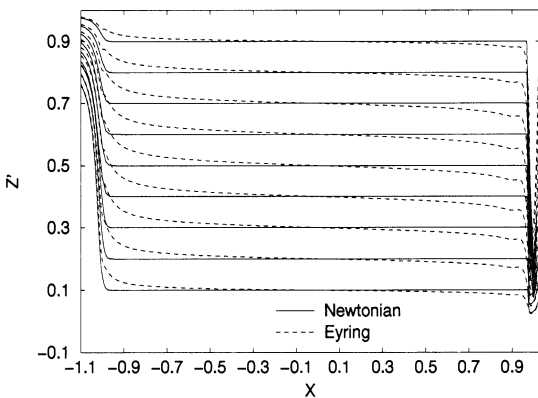
Fig. 11 Isovelocity lines across and through the contact for the Newtonian and Eyring models in the smooth case ($\mathscr{S} = 1$)

defined and measured at $X = 0$ will show the same trend as at the inlet, a monotonic increase with $\mathscr{S}$.

In the non-Newtonian case, by contrast, the steady increase in λ' with X implies a corresponding steady increase in amplitude *reduction* (decrease in amplitude). The initial ordering according to $\mathscr{S}$ seen in the inlet thus gives way to an ordering according to $|\mathscr{S}|$ as the centre of the contact is approached. This accounts for the almost symmetrical form of the present $\mathscr{A}_\mathrm{d}/\mathscr{A}_\mathrm{i}(X = 0)$ versus $\mathscr{S}$ plots, in sharp contrast with the steadily increasing plots for the Newtonian case [9]. The deviations of these plots from a smooth curve, termed 'variations' in reference [9], are due to the interference between the 'original' waviness of wavelength λ and the 'induced' waviness of wavelength λ', an effect seen particularly clearly as a function of X in Figs 7 and 8.

5   CONCLUSIONS

Implementing a non-linear fluid model, amplitude reduction computations have been performed for different slide−roll ratios. The reduction in amplitude curves in the centre of the contact shows for both $\lambda = 0.5$ and $\lambda = 1.0$ an increase with increasing $\mathscr{S}$ when $\mathscr{S} < 0$ followed by a decrease with increasing $\mathscr{S}$ for $\mathscr{S} > 0$. A closer look at the deformation of the waviness throughout the contact shows that in the central region the relative amplitude $\mathscr{A}_\mathrm{d}/\mathscr{A}_\mathrm{i}$ decreases from the inlet to the outlet. On this downward slope, oscillations are superimposed which become more important when the slip magnitude is increased and the wavelengths are small.

The effect of the Poiseuille flow on the velocity profile is thought to be the basis of this behaviour. The lubricant accelerates throughout the contact, regardless of the position of the fastest-moving surface, which is either the upper or the lower surface. The link between the velocity and the wavelength [equation (11)], and thus amplitude reduction may then be used to explain this symmetrical behaviour. Comparison of these results with calculations of amplitude reduction using the Newtonian model shows that a non-Newtonian model should be used whenever loads are high and in the presence of slip.

Finally, the significant variations in the amplitude reduction throughout the contact require that the behaviour of the waviness throughout the entire contact be monitored. Further research has to be done to find another parameter to replace the amplitude reduction as defined by Venner *et al*. [8], which would take these variations into account.

REFERENCES

1 Jacobson, B. and **Hamrock, B. J.** Non-Newtonian fluid model incorporated into elastohydrodynamic lubrication of rectangular contacts. *Trans. ASME, J. Tribology*, 1984, **106**(2), 275−284.

2 Conry, T. F., Wang, S. and **Cusano, C.** A Reynolds−Eyring equation for elastohydrodynamic lubrication in line contacts. *Trans. ASME, J. Tribology*, 1987, **109**, 648−658.

3 Lee, R.-T. and **Hamrock, B. J.** A circular non-Newtonian model. Part 1: used in elasto-hydrodynamic lubrication. *Trans. ASME, J. Tribology*, 1990, **112**, 386−496.

4 Iivonen, H. and **Hamrock, B. J.** A new non-Newtonian fluid model for elastohydrodynamic lubrication of rectangular contacts. *Wear*, 1991, **143**, 297−305.

5 Ai, X. and **Zheng, L.** A genreal model for micro-elastohydrodynamic lubrication and its full numerical solution. *Trans. ASME, J. Tribology*, 1989, **111**, 569−576.

6 Chang, L., Cusano, C. and **Conry, T. F.** Effects of lubricant rheology and kinematic conditions on micro-elastohydrodynamic lubrication. *Trans. ASME, J. Tribology*, 1989, **111**, 344−351.

7 Chang, L., Webster, M. N. and **Jackson, A.** On the pressure rippling and roughness deformation in elastohydrodynamic lubrication of rough surfaces. *Trans. ASME, J. Tribology*, 1993, **115**, 439−444.

8 Venner, C. H., Couhier, F., Lubrecht, A. A. and **Greenwood, J. A.** Amplitude reduction of waviness in transient EHL line contacts. In *Elastohydrodynamics '96*, Proceedings of the 23rd Leeds−Lyon Symposium on *Tribology* (Eds D. Dowson, C. M. Taylor, T. H. C. Childs, G. Dalmaz, Y. Berthier, L. Flamand, J.-M. Georges and A. A. Lubrecht), September 1996, 1997, pp. 103−112 (Elsevier, Amsterdam).

9 Lubrecht, A. A., Graille, D., Venner, C. H. and **Greenwood, J. A.** Waviness amplitude reduction in EHL line contacts under rolling sliding. *Trans. ASME, J. Tribology*, 1998, **120**, 705−710.

10 Johnson, K. L. Non-Newtonian effects in elastohydrodynamic lubrication. In Proceedings of the 19th Leeds−Lyon Symposium on *Tribology* (Eds D. Dowson, C. M. Taylor and M. Godet), Leeds, September 1992, 1993, pp. 15−26 (Elsevier, Amsterdam).

11 Johnson, K. L. and **Tevaarwerk, J. L.** Shear behaviour of elastohydrodynamic oil films. *Proc R. Soc. Lond. A*, 1977, **356**(12), 215−236.

12 Evans, C. R. and **Johnson, K. L.** The rheological properties of elastohydrodynamic lubricants. *Proc. Inst Mech. Engrs, Part C, Journal of Mechanical Engineering Science*, 1986, **200**(C5), 303−312.

13 Dowson, D. and **Higginson, G. R.** *Elasto-hydrodynamic Lubrication, the Fundamentals of Roller and Gears Lubrication*, 1966 (Pergamon, Oxford).

14 Roelands, C. J. A. Correlational aspects of the viscosity-temperature-pressure relationship of lubricating oils. PhD thesis, Technische Hogeschool Delft, The Netherlands (VRB, Groningen).

15 Lubrecht, A. A., Ten Napel, W. E. and **Bosma, R.** Multigrid, an alternative method for calculating film thickness and pressure profiles in elastohydrodynamically lubricated line contacts. *Trans. ASME, J. Tribology*, 1986, **108**, 551−556.

16 Brandt, A. and **Lubrecht, A. A.** Multilevel matrix multi-

plication and fast solution of integral equations. *J. Comput. Phys.*, 1990, **90**, 348–370.

17 Venner, C. H. Multilevel solution of the EHL line and point contact problems. PhD thesis, University of Twente, Enschede, The Netherlands.

18 Venner, C. H. and **Lubrecht, A. A.** Transient analysis of surface feature in an EHL line contact in case of sliding. *Trans. ASME, J. Tribology*, 1994, **116**, 186–193.

19 Greenwood, J. A. and **Morales-Espejel, G. E.** The behaviour of transverse roughness in EHL contacts. *Proc. Instn Mech. Engrs, Part J, Journal of Engineering Tribology*, 1994, **208** (J2), 121–132.

20 Hooke, C. J. Surface roughness modifications in elastohydrodynamic line contacts operating in the elastic piezoviscous regime. *Proc. Instn Mech. Engrs, Part J, Journal of Engineering Tribology*, 1998, **212**(J2), 145–162.

21 Lubrecht, A. A. Influence of local and global features in EHL contacts. In *Elastohydrodynamics '96*, Proceedings of the 23rd Leeds–Lyon Symposium (Eds D. Dowson, C. M. Taylor, T. H. C. Childs, G. Dalmaz, Y. Berthier, L. Flamand, J.-M. Georges and A. A. Lubrecht), September 1996, 1997, pp. 17–25 (Elsevier, Amsterdam).